# APPENDIX A

# SENSORS

## A.1 Piezoelectric accelerometer

*Table A.1: Specifications of the miniature (M352C22) and lightweight (M353B65) accelerometer used*

| Decription | Units | M352C22 | 353B65 |
|---|---|---|---|
| Voltage sensitivity | $mV/ms^{-2}$ | 10 | 100 |
| Frequency range (±5%) | Hz | 5 to 8000 | 1 t o10000 |
| Resonant frequency | kHz | >32 | >70 |
| Amplitude range | $\pm m/s^2$ pk | 500 | 50 |
| Mechanical shock limits | $\pm m/s^2$ pk | 0.0015 | 0.007 |
| Temperature range | °C | -31 to +121 | -31 to 121 |
| Amplitude linearity | % | ±1 | ±1 |
| Transverse sensitivity | % | <5 | <5 |
| Base strain sensitivity | $m/s^2/\mu_\varepsilon$ | <0.05 | <0.002 |
| Excitation voltage | VDC | 18 to 30 | 18 to 30 |
| Constant current excitation | mA | 2 to 20 | 2 to 20 |
| Discharge time constant | second | >0.3 | >0.5 |
| Sensing element | type | ceramic | quartz |
| Weight | gram | 0.5 | 2 |

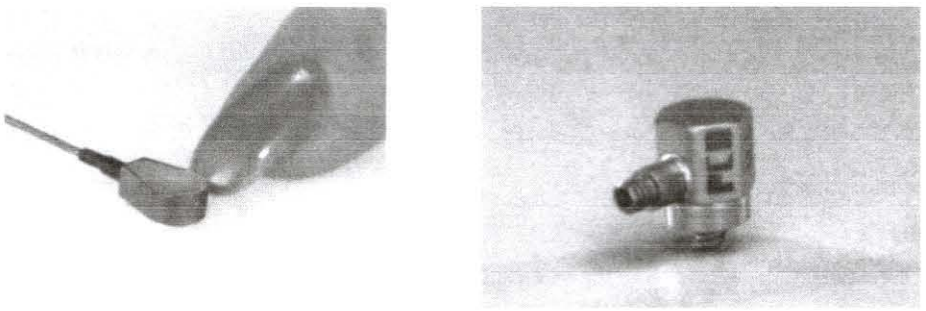

*Figure A.1: Miniature (left) and lightweight (right) accelerometer available.*

These are just two of the many types of accelerometers available of the shelf. The miniature accelerometer cost around R5000 and will work very well for this application. The lightweight accelerometer provides better sensitivity and also worked adequately for this application. Specifications can be seen in table A.1.

## A.2 Piezoelectric strain gauge

*Fig A.2: The PCB piezoelectric strain gauges used on the EFBDS.*

The piezoelectric strain gauges are ideal sensors for the measurement of system dynamics. The very low weight and profile makes for easy attachment with adhesives and minimal turbulence in fan systems. Due to the position of maximum strain being at the root of the blade, these sensors are also not subjected to maximum flow velocities, a problem for accelerometers. Specifications can be seen in table A.2.

*Table A.2: Specifications for piezoelectric strain gauge (*740B02)

| Description | Value |
|---|---|
| Sensitivity (±20 %) | 50 mV/μ E |
| Amplitude range | 100 peak/μ E |
| Broadband resolution (1 Hz to 10 kHz) | 0.6 μ E |
| Frequency range | 0.5 to 100 000 Hz |
| Operating temperature range | -53 to +121 °C |
| Output bias | 9to 13 VDC |
| Cable, 3m length supplied | Integral Coaxial |
| Weight | 0,5 grams |
| Size (Width x Length x Height) | 5,1 x 15,2 x 1,8 mm |

# APPENDIX B

## Work drawing of Majuba fan blade

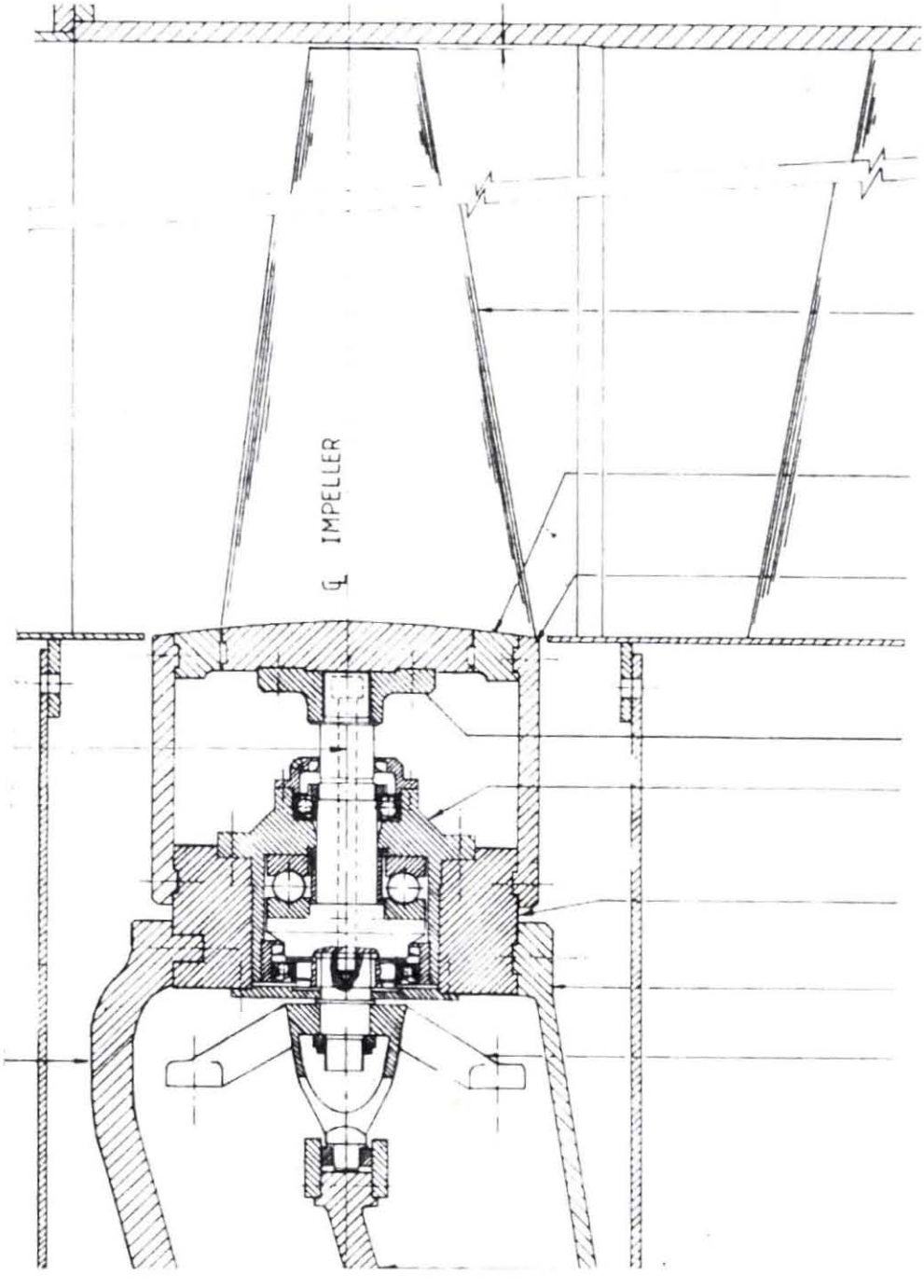


*Fig B.1: Section drawing of one of the fan blades of the FD fan at Majuba*

# APPENDIX C

## INVESTIGATION OF ARMAX MODELLING TECHNIQUE

### C.1 Experimental test structure

To evaluate the effectiveness of using an ARMAX model to determine natural frequencies of a system, a simple aluminium cantilever beam was used. A schematic of the experimental test set-up can be seen in figure C.1.

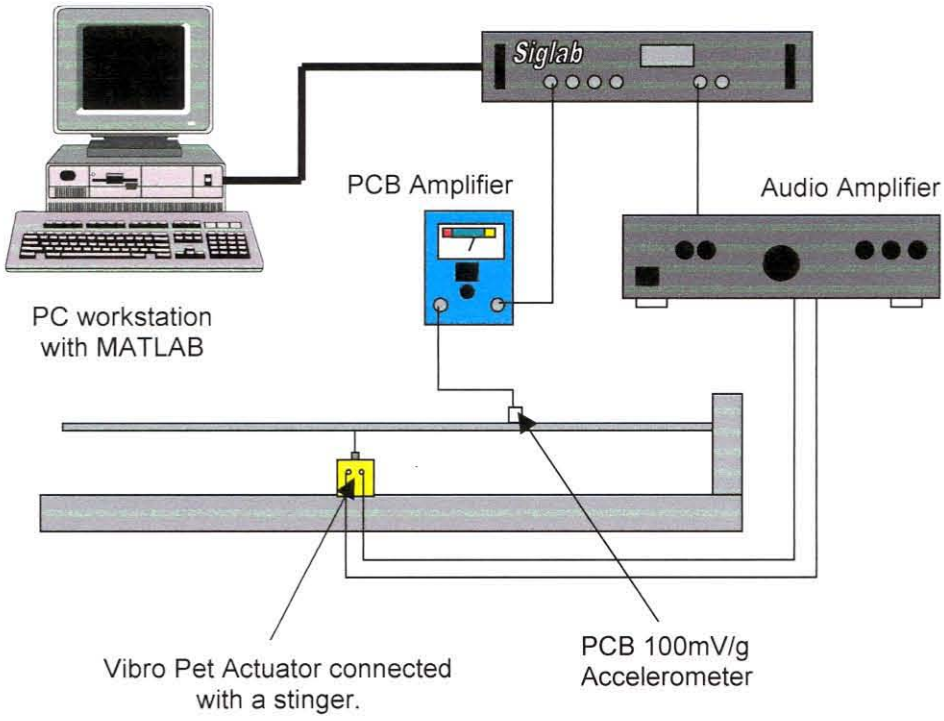


*Figure C.1: Schematic of the experimental test structure used to verify the ARMAX technique*

Since no input on the experimental fan blade damage simulator was going to be available, only the output from the accelerometer mounted on the aluminium cantilever beam was used to determine a suitable ARMAX model. A random stochastic signal with a 0-500Hz bandwidth was generated by the *Siglab* analyser to excite the beam. This signal was amplified using an audio amplifier. Due to the poor performance of the audio amplifier below 20Hz, the first natural frequency of the beam

(around 9Hz) was not excited properly and no attempt was made to correctly identify this frequency.

A typical time signal obtained from the validation model can be seen in figure C.2. The signal was filtered with a bandpass filter of 5Hz to 560 Hz and calibrated to give acceleration in $m/s^2$.

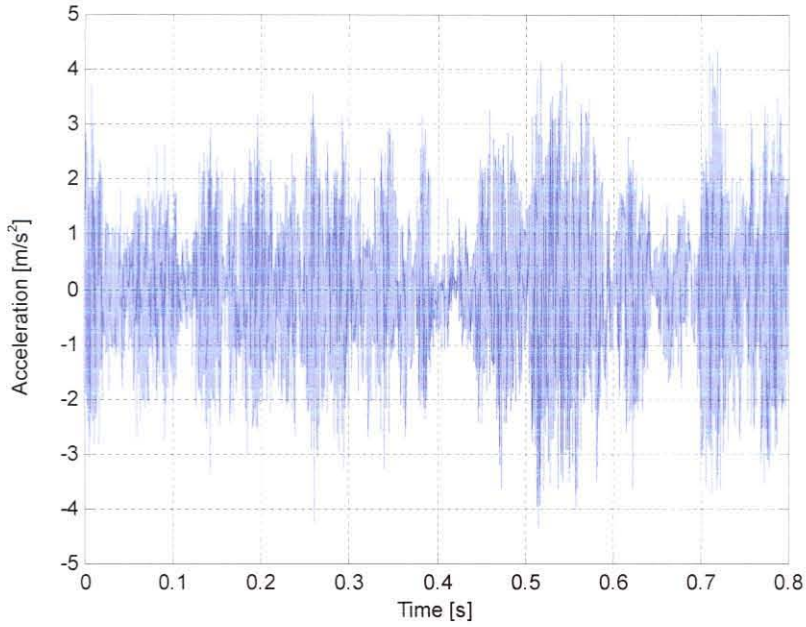


*Figure C.2: Typical time signal (filtered and calibrated)*

## C.2 The effect of signal length

Since the ARMAX modelling technique made use of time signals to fit a curve, the length of the samples could be varied. Figure C.3 shows the typical power spectral densities and ARMAX curve fits for various sampling lengths, while tables C.1 through C.4 show the second, third and fourth natural frequencies found by means of a peak picking method on the ARMAX fit.

*Table C.1: 0.8s sampling time results*

| Natural frequencies | $f_3$ (±63.7 Hz) | $f_3$ (±176.7 Hz) | $f_4$ (±332 Hz) |
|---|---|---|---|
| Measurement 1 | 59.41 | 173.61 | 320.78 |
| Measurement 2 | 59.16 | 173.98 | 320.09 |
| Measurement 3 | 59.54 | 173.98 | 320.09 |
| Measurement 4 | 60.45 | 172.86 | 318.71 |

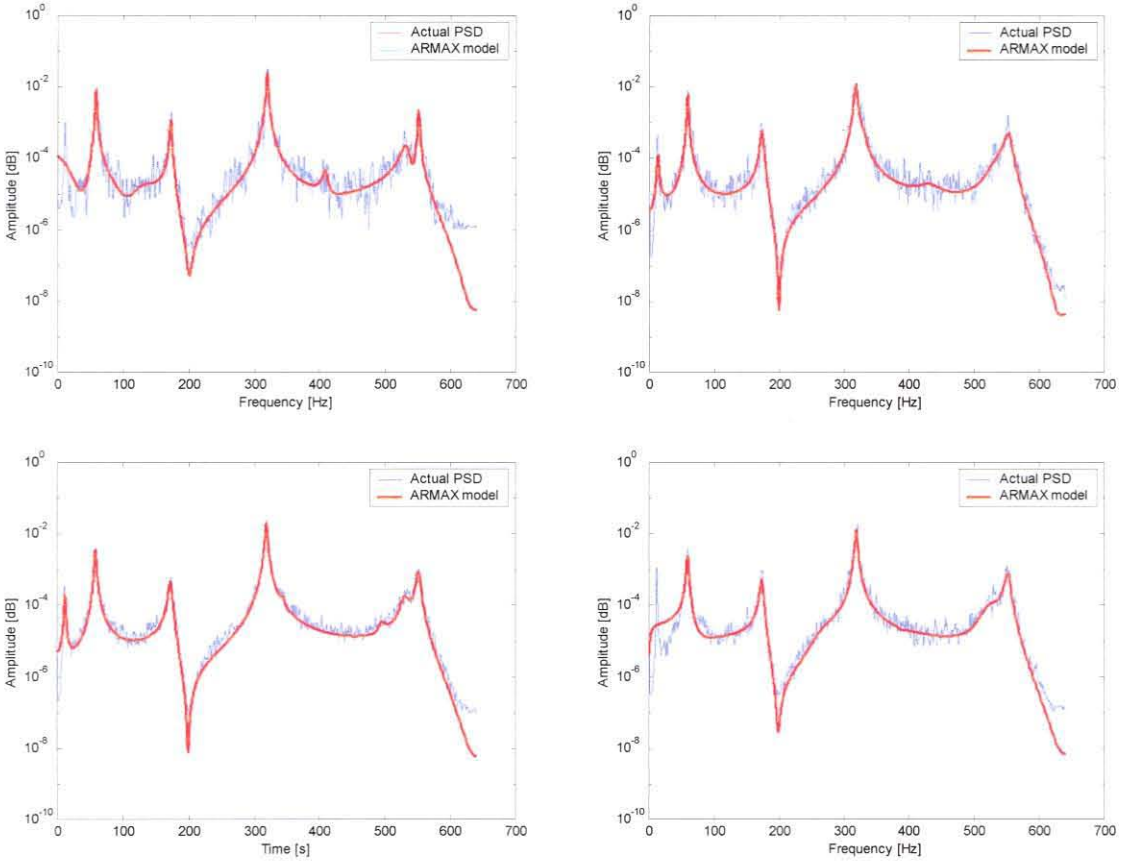


*Figure C.3: Typical fits for, from top left clockwise, 0.8s, 1.6s, 3.2s and 6.4s samples.*

It was readily apparent that a smoother PSD was obtained with longer sample lengths. This could be expected. Interestingly enough, the curve fits obtained provided accurate natural frequencies results even with shorter samples.

*Table C.2: 1.6 s sampling time results*

| Natural frequencies | $f_3$ (≈63.7 Hz) | $f_3$ (≈176.7 Hz) | $f_4$ (≈332 Hz) |
|---|---|---|---|
| Measurement 1 | 59.93 | 174.36 | 318.71 |
| Measurement 2 | 59.41 | 173.98 | 318.71 |
| Measurement 3 | 59.54 | 173.61 | 320.09 |
| Measurement 4 | 60.19 | 173.98 | 320.09 |

*Table C.3: 3.2 s sampling time results*

| Natural frequencies | $f_3$ (≈63.7 Hz) | $f_3$ (≈176.7 Hz) | $f_4$ (≈332 Hz) |
|---|---|---|---|
| Measurement 1 | 60.06 | 174.36 | 319.40 |
| Measurement 2 | 60.06 | 173.61 | 319.40 |
| Measurement 3 | 59.80 | 173.48 | 318.71 |
| Measurement 4 | 59.80 | 173.98 | 318.71 |

*Table C.4: 6.4 s sampling time results*

| Natural frequencies | $f_3$ (≈63.7 Hz) | $f_3$ (≈176.7 Hz) | $f_4$ (≈332 Hz) |
|---|---|---|---|
| Measurement 1 | 59.28 | 173.61 | 318.71 |
| Measurement 2 | 59.41 | 173.61 | 320.09 |
| Measurement 3 | 59.33 | 173.98 | 319.40 |
| Measurement 4 | 59.54 | 173.61 | 319.40 |

A comparison of the accuracy can be seen if figure C.4.

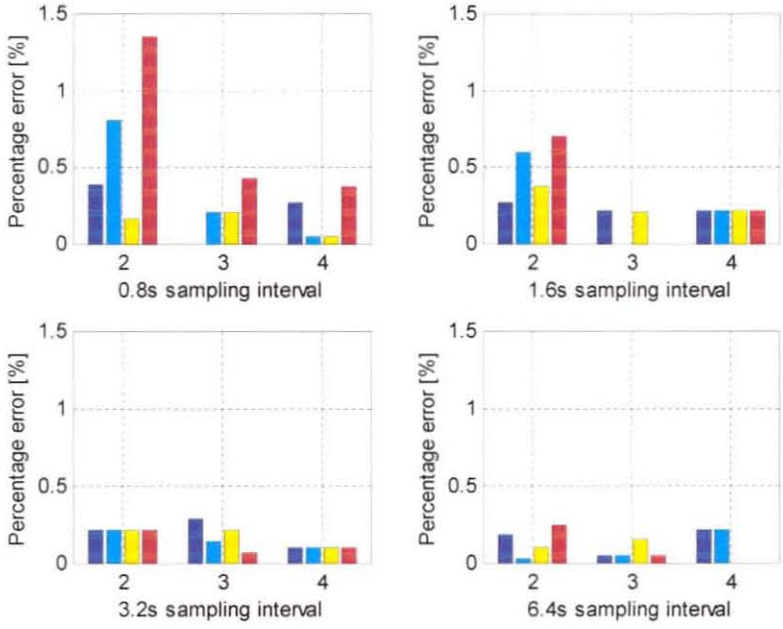


*Figure C.4: Increasing accuracy with longer sampling times*

While longer samples were the most accurate, the processing time did go up as the sample length increased. Table C.5 shows the processing time in seconds used for the four different sampling times ($12^{th}$ order ARMAX models were used throughout).

*Table C.5: Comparison of processing times for different sampling intervals.*

| Description | Central Processing Unit (CPU) time |
|---|---|
| 0.8 second sampling interval | 2.64 s |
| 1.6 second sampling interval | 3.79 s |
| 3.2 second sampling interval | 5.66 s |
| 6.4 second sampling interval | 13.96 s |

These times included loading of data and the ARMAX subroutine and were the average of 4 runs on the same data file. The computer was a Pentium II ™ 350MHz with 128 MB of RAM.

## C.3 Effect of model order

An order for the polynomial curve fit that the ARMAX subroutine fits through time domain data had to be specified. It is very difficult to compute an order for output only data. Curve fits of the $4^{th}$, $8^{th}$, $12^{th}$ and $16^{th}$ order can be seen in figure C.5. Clearly a certain minimum (12 in this case) was necessary to identify all the natural frequencies of the system.

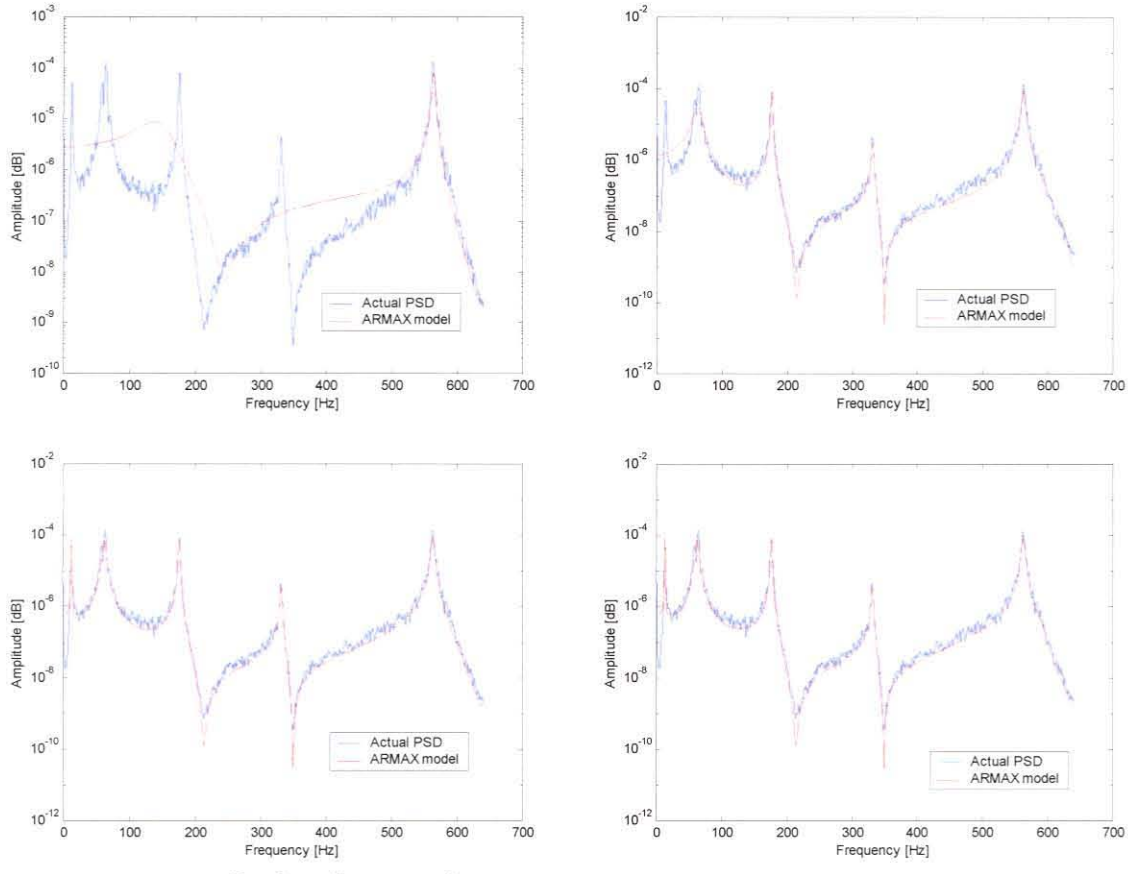


*Figure C.5: $4^{th}$, $8^{th}$, $16^{th}$, and $12^{th}$ order ARMAX models (from the top left clockwise)*

Once all the natural frequencies had been found and fitted with a curve however, the remaining orders model noise. This resulted in unnecessary CPU time and inaccuracies in the model. CPU times can be seen in table C.6.

*Table C.6: Comparison of processing times for different sampling intervals.*

| Description | Central Processing Unit (CPU) time |
|---|---|
| $4^{th}$ order ARMAX model | 4.78 s |
| $8^{th}$ order ARMAX model | 3.57 s |
| $12^{th}$ order ARMAX model | 5.66 s |
| $16^{th}$ order ARMAX model | 11.51 s |

The best way to determine if too high an order was used, consisted of calculating the poles and zeros of the ARMAX model. A comparison between $4^{th}$, $8^{th}$, $12^{th}$ and $16^{th}$ order fits can be seen if figures C.6 and C.7.

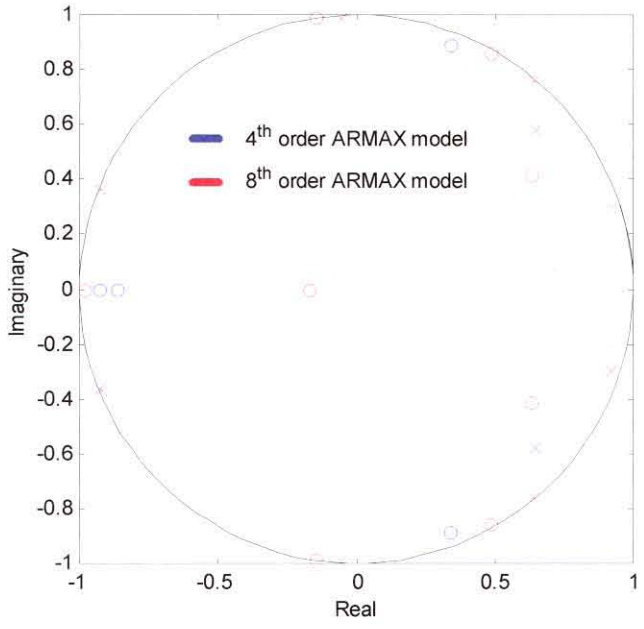


*Figure C.6: The pole-zero plots for different order ARMAX models.*

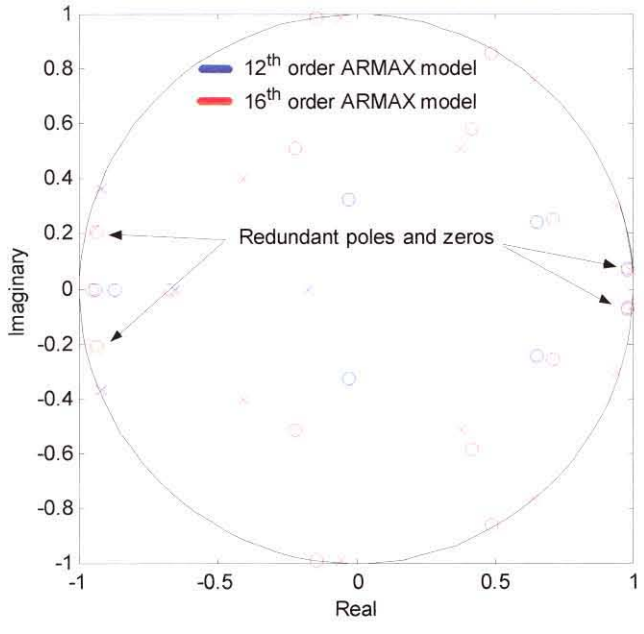


*Figure C.7: Too high an order results in redundant poles and zeros*

If poles and zeros coincide the system is over determined and redundant poles and zeros exist.

# APPENDIX D

# TYPICAL RESULTS FOUND

*Table D.1: Frequency shifts for various channels and operating conditions*

| 3rd natural frequency variation with increasing amounts of damage. | | | | | |
|---|---|---|---|---|---|
| **Description** | **0%** | **10%** | **20%** | **30%** | **40%** |
| Ch 1, 450 r.p.m, 500hz sampling frequency | 284.72 | 279.96 | 275.64 | 271.38 | 266.5 |
| Ch 2, 750 r.p.m, 1000hz sampling frequency | 280.13 | 274.10 | 268.38 | 268.00 | 262.97 |
| Ch 2, 750 r.p.m, 2000hz sampling frequency | 278.87 | 277.93 | 268.42 | 267.81 | 262.89 |
| Ch 3, 450 r.p.m, 500hz sampling frequency | 284.72 | 279.96 | 274.57 | 270.68 | 266.5 |
| Ch 3, 750 r.p.m, 500hz sampling frequency | 279.96 | 279.6 | 274.92 | 270.68 | 266.5 |
| Ch 4, 450 r.p.m, 1000hz sampling frequency | 280.92 | 279.74 | 274.67 | 270.46 | 266.31 |

*Table D.2: Frequency shifts for various channels and operating conditions*

| 4th natural frequency variation withincreasing amounts of damage. | | | | | |
|---|---|---|---|---|---|
| **Description** | **0%** | **10%** | **20%** | **30%** | **40%** |
| Ch 1, 450 r.p.m, 500hz sampling frequency | 435.68 | 435.68 | 435.68 | 436.25 | 436.25 |
| Ch 2, 750 r.p.m, 1000hz sampling frequency | 446.97 | 446.34 | 444.15 | 440.42 | 436.72 |
| Ch 2, 750 r.p.m, 2000hz sampling frequency | 446.67 | 446.16 | 444.14 | 440.46 | 436.48 |
| Ch 3, 450 r.p.m, 500hz sampling frequency | 446.55 | 446.55 | 444.24 | 440.8 | 436.81 |
| Ch 3, 750 r.p.m, 500hz sampling frequency | 446.55 | 446.55 | 444.24 | 440.8 | 436.81 |
| Ch 4, 450 r.p.m, 1000hz sampling frequency | 447.28 | 446.34 | 444.15 | 440.42 | 440.42 |

*Table D.3: Frequency shifts for the finite element model.*

| **Finite element model 3rd natural frequency variation with increasing amounts of damage.** | | | | | |
|---|---|---|---|---|---|
| **Description** | **0%** | **10%** | **20%** | **30%** | **40%** |
| 450 r.p.m. 1240 elements | 284.85 | 283.097 | 268.863 | 245.229 | 213.756 |
| 750 r.p.m, 1240 elements | 285.018 | 283.266 | 268.978 | 245.352 | 213.992 |
| **Finite element model 4th natural frequency variation with increasing amounts of damage.** | | | | | |
| 450 r.p.m. 1240 elements | 434.932 | 434.023 | 431.429 | 427.463 | 421.905 |
| 750 r.p.m, 1240 elements | 435.132 | 434.226 | 431.588 | 427.624 | 422.146 |